Time-Frequency Analysis on Numerical and Experimental Ultrasonic Guided Wave Scattering for Quantitative Damage Characterization in Plates

MINGYUE ZHANG, JANELLE COLEEN DELA CUEVA, HYONNY KIM and MARGHERITA CAPRIOTTI

ABSTRACT

Ultrasonic guided waves (UGWs) have been proven to be an effective technique for structural health monitoring (SHM) due to their low attenuation and high sensitivity to defects across the entire structural cross-section, outperforming conventional inspection methods. However, the dispersive and multi-mode nature of UGWs presents significant challenges for structural inspection, limiting their effectiveness in damage detection and characterization. The interaction between different mode-frequency combinations and structural defects, such as delaminations and notches, affects UGW scattering according to complex mechanisms that challenge inspection techniques. Therefore, a deeper understanding of the distinct scattering phenomena with respect to defect types and sizes is essential for improving the diagnostics and prognostics of damage.

In this study, numerical and experimental methods are employed to analyze UGW interactions with plate-like structures in both the time- and frequency- domains. First, the hybrid Global-Local method is used to simulate UGW propagation in isotropic and composite plates with defects of varying types and sizes. This enables a comprehensive investigation of the wave-damage interaction over a broad frequency range. Then, experimental testing is performed to observe and validate the numerical findings, using broadband guided wave testing. Signal processing is applied in the time and frequency domain to extract transfer and impulse response functions via the deconvolution method. The results from the numerical simulations reveal amplitude, time shifting and frequency content alterations that align with the experimental tests and that vary with defect type and severity, providing valuable insights for effective SHM applications.

These studies demonstrate the effectiveness of the Global-Local approach in enabling quantitative SHM and prognostics by providing accurate and efficient predictions of UGW scattering responses. Furthermore, the distinct scattering behavior observed for different defect types and sizes highlight the potential of leveraging these features to solve the inverse problem of defect characterization.

Mingyue Zhang, Joint PhD Student, Email: mzhang4113@sdsu.edu. Department of Aerospace Engineering, San Diego State University, San Diego, CA, and Department of Structural Engineering, University of California San Diego, La Jolla, CA, USA
Janelle Coleen Dela Cueva, PhD Student, Email: jcdelacu@ucsd.edu. Department of Structural Engineering, University of California San Diego, La Jolla, CA, USA
Dr. Hyonny Kim, Professor, Email: hyk015@ucsd.edu. Department of Structural Engineering, University of California San Diego, La Jolla, CA, USA
Dr. Margherita Capriotti, Assistant Professor, Email: mcapriotti@sdsu.edu. Department of Aerospace Engineering, San Diego State University, San Diego, CA, USA

INTRODUCTION

Structural Health Monitoring (SHM) plays a crucial role in ensuring the safety and reliability of engineering structures by enabling the early detection and characterization of defects. Among various SHM techniques, Ultrasonic Guided Waves (UGWs) have attracted significant attention due to their ability to propagate over long distances with minimal attenuation, penetrate through the entire structural thickness, and exhibit high sensitivity to a wide range of defect types and sizes [1, 2]. These attributes make UGWs particularly suitable for inspecting plate-like structures commonly used in aerospace, mechanical, marine, energy and transportation engineering applications [3].

However, accurately modeling the interaction of UGWs with structural defects presents substantial challenges. Traditional full-size Finite Element (FE) models are computationally demanding, especially when simulating wave propagation over large domains or across broadband frequency ranges. This challenge becomes even more pronounced in the case of complex materials such as composites, which exhibit anisotropic and multilayer properties.

To address these limitations, hybrid modeling approaches have been developed to optimize computational efficiency while maintaining accuracy. One such approach is the hybrid Global-Local (GL) method, which integrates Semi-Analytical Finite Element (SAFE) model for the global region with FE model for the defected local region. This method has been developed for 2D [4] and 3D structures [5], and enhanced for forced response analysis [6, 7], evanesecent modes inclusion [8], and scattering spectra prediction [9]. The GL method has demonstrated accuracy and efficiency for simulating UGW propagation and scattering in structures with localized anomalies.

In this study, the hybrid GL method is employed to investigate UGW interactions with structural defects in both isotropic aluminum and composite plates. The transient response induced by broadband UGW scattering is computed and analyzed. Numerical results are validated through experimental testing using broadband guided wave excitation and reception. Time-frequency deconvolution is used to extract transfer and impulse responses, enabling comparison. The results confirm the method's potential for quantitative damage characterization in SHM.

HYBRID GLOBAL-LOCAL METHOD

The numerical investigation conducted in this study employs the hybrid Global-Local method to analyze ultrasonic guided wave (UGW) interaction with structural defects in both isotropic and composite plate-like structures. The Global-Local method integrates the Semi-Analytical Finite Element (SAFE) global solutions with local Finite Element (FE) analyses, ensuring continuity in displacements and tractions at the interface boundaries.

The schematic illustration of the two-dimensional scattering problem addressed by this method is presented in Fig. 1. A detailed formulation can be found in the literature [4]. The computational framework employed in this study was enhanced with specialized subroutines developed for forced UGW scattering analyses [7].

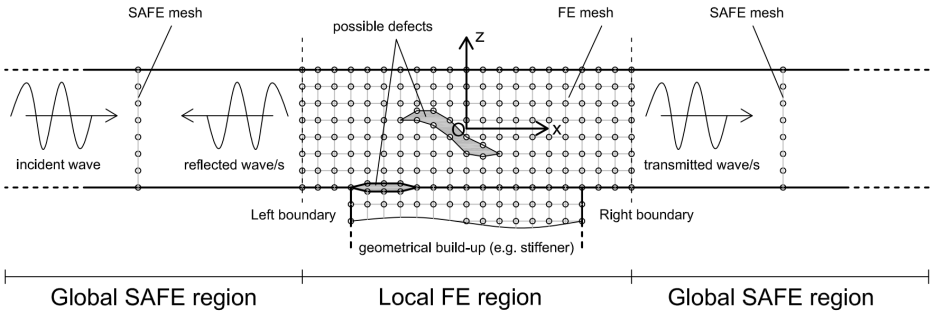

Figure 1. Geometrical representation of the scattering of an incident wave in reflected and transmitted waves from a local zone (LZ), with indication of the adopted discretization strategies in each region of the Global-Local approach [4].

To demonstrate the accuracy and effectiveness of the hybrid Global-Local method, two distinct material scenarios—an isotropic aluminum plate and a multilayer composite plate—were numerically modeled and experimentally validated. Each scenario involves unique structural defect configurations and experimental setups, providing comprehensive insights into the interaction of ultrasonic guided waves (UGWs) with various defects across different materials. These cases are discussed in detail in the subsequent sections.

CASE STUDY: ISOTROPIC ALUMINUM PLATE

Numerical Modeling

In the first scenario, an isotropic aluminum plate was studied. The local region for aluminum plate was defined as a two-dimensional rectangular plate, 50 mm long and 2 mm thick. To ensure numerical accuracy and convergence, a fine mesh consisting of linear quadrilateral elements with four Gauss points per element was used, adopting an element size of 0.05 mm, which guarantees more than 20 finite elements per wavelength. Several structural configurations were analyzed, including a pristine plate, plates with notches of varying depths (1 mm and 1.5 mm), and a plate with a through-thickness defect. Both notch and through-thickness defects have a consistent width of 1.5 mm.

The dispersion curves for the aluminum plate, obtained from the SAFE analysis of the Global-Local method, are presented in Fig. 2 (a) for frequencies ranging from 0 to 500 kHz. A consistent forcing function was applied to both pristine and damaged cases. A single-input dual-output (SIDO) setup was utilized: the source was positioned 0.20 m to the left from the center of the local zone, and Receiver 1 (R1) was placed 0.10 m to the right from the source, before the defect, while Receiver 2 (R2) was placed at 0.30 m to the right from the source, beyond the defect, as schematically illustrated in Fig. 2 (b).

A Gaussian pulse, as detailed in [10], served as incident waveform, covering a broadband frequency range up to 500 kHz. The spatial force was applied by a pure A0 mode at the source location. This setup operated at a sampling frequency of 1 MHz, with a frequency resolution of 1 kHz. The out-of-plane displacement responses at the surface nodes on locations corresponding to receivers R1 and R2, resulting from the Gaussian pulse excitation, were recorded.

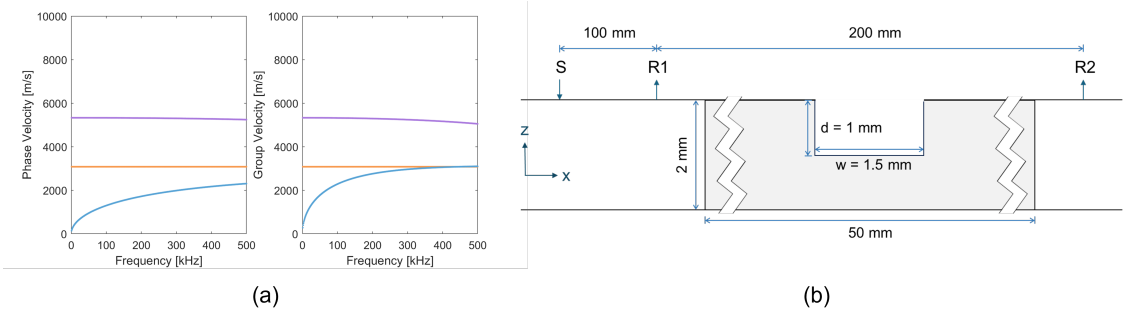

Figure 2. a) Dispersion curves for the 2 mm thick aluminum plate; b) schematic illustration of the single-input dual-output (SIDO) setup in the aluminum plate featuring a notch (depth d = 1 mm, width w = 1.5 mm).

Deconvolution was employed to extract the transfer function or Green's function between the two receivers. In the SIDO configuration, the portion of the structure between two receivers is the inspection region of interest. By isolating the transfer function G_{R1R2}, characteristics of the targeted region can be analyzed independently from source excitation effects and boundary reflections, as detailed in previous studies [11–15]

The transfer function in the frequency domain was obtained by deconvolving the signal at R1 from that at R2. Subsequently, the impulse response was computed through inverse Fourier transformation. A Hanning window was utilized to filter the signal within the frequency range of 0 – 200 kHz to align with experimental test results. The filtered transfer function in frequency domain and impulse response in time domain between R1 and R2 are illustrated in Fig. 3 (a). The results have been normalized to the maximum absolute amplitude of the pristine result to allow comparison with the experimental results.

In the frequency domain results, the amplitude of the transfer function progressively decreases as the defect depth increases, due to a reduction in transmitted energy. Specifically, for the through-thickness defect, the transmitted signal is absent at R2, indicating

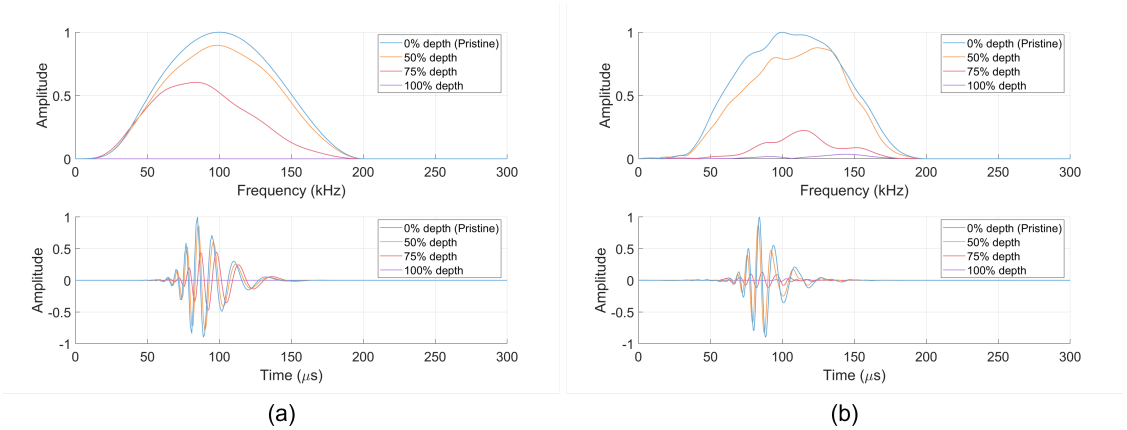

Figure 3. Normalized transfer functions (frequency domain) and impulse responses (time domain) measured between receivers R1 and R2 for isotropic aluminum plates: a) numerical Global-Local results; b) experimental results. Plate conditions: pristine (blue), 1 mm notch (orange), 1.5 mm notch (rose), through-thickness defect (purple).

complete reflection at the defect. When the notch exceeds half the plate thickness (1.5 mm), a notable drop in transfer function amplitude occurs for frequencies above approximately 65 kHz. In the corresponding impulse responses, the pristine aluminum plate exhibits a dispersive waveform and a clear maximum at approximately 84.83 μs. As the notch depth increases, this peak amplitude shifts slightly to a later time. Although the impulse response amplitude for the 1 mm notch (half-thickness) remains similar to the pristine condition with slightly reduced amplitude, the amplitude significantly decreases less than 50% of the pristine amplitude once the notch depth reaches 1.5 mm. Ultimately, when the defect becomes a through-thickness, no transmitted energy is observed after the defect location.

Experimental Validation

To support and validate the numerical simulations, experimental tests were conducted utilizing the same SIDO system setup (Fig. 2 (b)). UGWs were generated using a in-house manufactured mini-impactor, capable of generating broadband signals spanning frequencies from 40 to 500 kHz [16]. Signal acquisition was performed using two broadband contact piezoelectric transducers (Picosensors, Mistras), designated as R1 and R2, positioned identically to the numerical receiver locations.

The deconvolution method, assuming identical receiver responses, was applied to the experimental signals at R1 and R2 to extract the transfer and impulse response functions, as shown in Fig. 3(b). The experimental transfer function shows a notable amplitude decrease as defect depth increases, consistent with numerical predictions. However, the experimental frequency response exhibits some variations along the frequency range compared to the numerical results. This is attributed to transducers and source response, and boundary reflections. In the presence of a through-thickness defect, the experimental data retains a small residual amplitude (below 4%), likely due to wave reflections from the defect edges or plate boundaries, as evident in the impulse response function. The peak amplitude in the experimental impulse response occurs at approximately 84 μs, aligning closely with numerical estimation. Similar to numerical findings, deeper defects result in decreased impulse response amplitudes and slight time shifts. It should also be noted that the experimental results demonstrate comparatively lower amplitudes, particularly for defects deeper than half the plate thickness.

CASE STUDY: COMPOSITE PLATE

Numerical Modeling

The second scenario investigates a composite plate made of AS4/977-3 prepreg material, with a total thickness of 1.85 mm and a $[0/90/0/90/0]_S$ layup. Elastic material properties used in the simulation align with those measured from the experimental specimens, as detailed in Table I. The local region length for the composite analysis remained at 50 mm, well beyond the recommended minimum distance (four times the plate thickness) between the local boundary and defect region [8]. The mesh configuration utilized linear quadrilateral elements with a refined mesh size of 0.04625 mm through the thickness direction (equivalent to four elements per ply thickness), and 0.05 mm in the wave

TABLE I. ELASTIC PROPERTIES OF THE COMPOSITE LAMINA

Property	C_{11}	C_{12}	C_{13}	C_{22}	C_{23}	C_{33}	C_{44}	C_{55}	C_{66}
GPa	150	5.37	5.37	13.5	6.43	13.5	3.52	5.78	5.78

propagation direction. Two composite configurations were examined: a pristine composite plate and a plate containing a symmetric delamination, measuring 12.7 mm in width, located centrally between the fifth and sixth lamina plies. The delamination was modeled by separating the finite element nodes at the lamina interface, creating an infinitesimal opening, as depicted in Fig. 4 (b).

Fig.4 (a) presents the dispersion curves for this composite plate within a frequency range of 0 to 500 kHz. The SIDO system configuration was adjusted to shorter inspection distances compared to the isotropic aluminum case, in order to accommodate the smaller size of the composite panel. Specifically, the source was positioned 0.095 m to the left from the center of the local region. R1 was placed 0.04 m right of the source, before the defect, and R2 was placed 0.15 m right of the source, after the defect, as in Fig.4 (b).

Normalized transfer functions and impulse responses (Fig. 5(a)) reveals subtle differences between the delaminated and pristine cases due to the delamination being infinitesimal and in a symmetric configuration. Both the transfer function and impulse response exhibits minor changes caused by the delamination. The impulse response displays a time delay and a minor reduction in amplitude for the delaminated configuration compared to the pristine case. The latter results in a waveform with time of arrival occurring at 62.87 µs, which demonstrates a dominant frequency content of 100 kHz, closely aligning with the 63.43 µs predicted from dispersion curves.

Experimental Validation

A 420 mm × 420 mm composite panel, matching the layup and material properties used in simulations, was fabricated for experiments. A delamination was introduced during the fabrication process by inserting Wrightlon 5200 P31 non-perforated release film between the central plies.

Experimental tests were performed using the same SIDO configuration (Fig.4 (b))

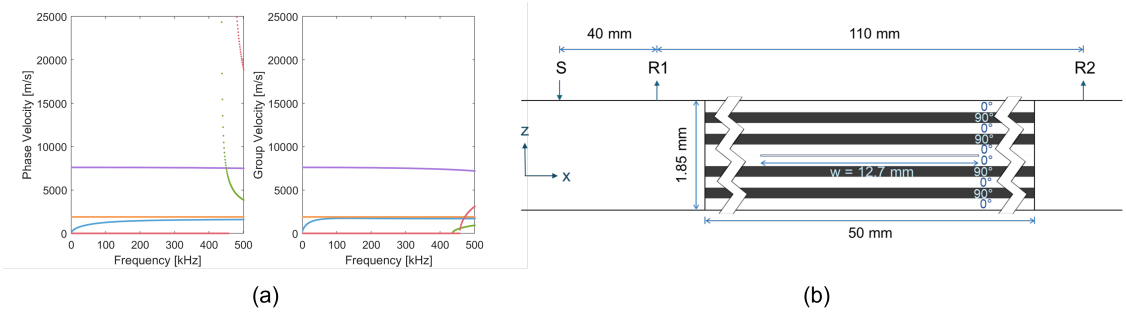

(a) (b)

Figure 4. a) Dispersion curves for the 1.85 mm thick composite plate; b) schematic illustration of the single-input dual-output (SIDO) setup, depicting broadband excitation and reception of the pure A0 mode in the composite plate featuring a symmetric delamination (width w = 12.7 mm).

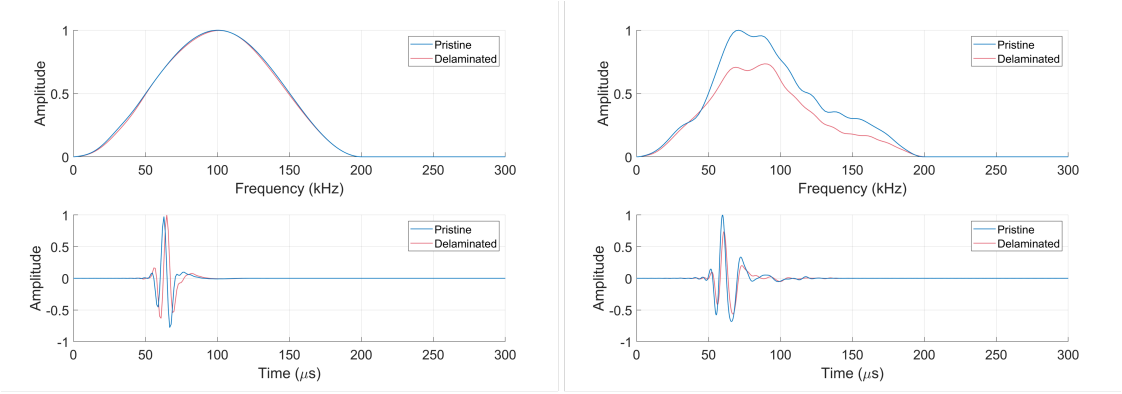

Figure 5. Normalized transfer functions (frequency domain) and impulse responses (time domain) measured between receivers R1 and R2 for composite plates: a) numerical Global-Local results; b) experimental results. Plate conditions: pristine (blue), 12.7 mm centered delamination (rose).

for both pristine and delaminated composite specimens. The normalized transfer and impulse response functions obtained from signals at receivers R1 and R2 are depicted in Fig. 5 (b). Experimental results show an observable reduction in amplitude for both transfer and impulse responses in the delaminated case compared to the pristine specimen. This amplitude reduction in the experimental results is more pronounced than that observed in the numerical predictions, primarily due to the higher attenuation induced by the teflon insert to reproduce delamination. The experimental impulse response peak appears at approximately 59.74 μs, matching numerical Global-Local predictions. Similar to the numerical outcomes, the experimental impulse response for the delaminated specimen demonstrates a subtle shift in time domain and reduced amplitude. Despite the large width of the delamination, the symmetric delamination geometry results in relatively moderate scattering effects in both numerical and experimental tests. The experimental results show a modified amplitude distribution along the frequency range in the transfer function with respect to the numerical results. This is attributed to the laminate's intrinsic characteristic and effects of mini-impactor and transducers responses.

CONCLUDING REMARKS

In this paper, the interaction of UGWs with structural defects in both isotropic aluminum and composite plates was investigated using a hybrid Global-Local method and validated by experimental analyses. The Global-Local approach enabled detailed analysis of wave propagation and scattering phenomena, providing insights into how defects of varying types and sizes influence UGW responses in different materials. Experimental validation using broadband guided wave testing and analysis further confirmed the predictive capabilities of the numerical method by extracting and analyzing transfer and impulse response functions through deconvolution. The accuracy and efficiency of this approach are confirmed, demonstrating its capability in predicting wave-defect interactions across different materials and defect configurations, in broadband inspection set-ups. The discrepancies observed between numerical simulations and experimental

results are primarily attributed to practical experimental challenges, including defect manufacturing imperfections and assumptions, edge and boundary reflections, and inconsistencies due to manually operated excitation methods. Additionally, limitations inherent to the Global-Local model used in this work, including two-dimensional modeling and exclusion of material viscoelasticity, were recognized. Future research will improve the method by developing a full three-dimensional numerical model incorporating evanescent modes, while maintaining computational efficiency. Additionally, future work will focus on quantitative damage characterization to advance SHM capabilities.

REFERENCES

1. Bartoli, I., A. Marzani, F. L. Di Scalea, and E. Viola. 2006. "Modeling wave propagation in damped waveguides of arbitrary cross-section," *Journal of sound and vibration*, 295(3-5):685–707.
2. Staszewski, W. J. 2004. "Structural health monitoring using guided ultrasonic waves," in *Advances in smart technologies in structural engineering*, Springer, pp. 117–162.
3. Rose, J. L. 2014. *Ultrasonic guided waves in solid media*, Cambridge University Press.
4. Spada, A., M. Capriotti, and F. L. di Scalea. 2020. "Global-Local model for guided wave scattering problems with application to defect characterization in built-up composite structures," *International Journal of Solids and Structures*, 182:267–280.
5. Spada, A., M. Capriotti, and F. Lanza di Scalea. 2022. "Global–local model for three-dimensional guided wave scattering with application to rail flaw detection," *Structural Health Monitoring*, 21(2):370–386.
6. CAPRIOTTI, M., M. ZHANG, L. ESCALONA, F. L. DI SCALEA, and A. SPADA. 2023. "Analyses by Global-Local Method of Ultrasonic Guided Waves Propagation in Pristine and Defective Plates for Accurate Quantitative SHM," *STRUCTURAL HEALTH MONITORING 2023*.
7. Capriotti, M., L. Escalona, and A. Spada. 2023. "Improved Global-Local Method for Ultrasonic Guided Wave Scattering Predictions in Composite Waveguides and Defects," *Journal of Nondestructive Evaluation, Diagnostics and Prognostics of Engineering Systems*, 6(4):041003.
8. Spada, A., M. Zhang, F. Lanza di Scalea, and M. Capriotti. 2023. "The role of evanescent modes in global-local analysis of ultrasonic guided waves in plates with varying local zone-scatterer relations," *Journal of Vibration and Control*:10775463231168926.
9. Zhang, M., L. W. E. Galvis, A. Spada, and M. Capriotti. 2024. "Ultrasonic Guided Wave Scattering Spectra by Hybrid Global–Local Modeling for Nondestructive Evaluation in Composites With Varying Defect Features," *Journal of Nondestructive Evaluation, Diagnostics and Prognostics of Engineering Systems*, 7(3):031001.
10. Wang, C. H., J. T. Rose, and F.-K. Chang. 2004. "A synthetic time-reversal imaging method for structural health monitoring," *Smart materials and structures*, 13(2):415.
11. Mueller, C. S. 1985. "Source pulse enhancement by deconvolution of an empirical Green's function," *Geophysical Research Letters*, 12(1):33–36.
12. Lanza di Scalea, F., X. Zhu, M. Capriotti, A. Y. Liang, S. Mariani, and S. Sternini. 2018. "Passive extraction of dynamic transfer function from arbitrary ambient excitations: Application to high-speed rail inspection from wheel-generated waves," *Journal of Nondestructive Evaluation, Diagnostics and Prognostics of Engineering Systems*, 1(1):011005–011005.
13. Capriotti, M. and F. Lanza di Scalea. 2020. "Robust non-destructive inspection of composite aerospace structures by extraction of ultrasonic guided-wave transfer function in single-input dual-output scanning systems," *Journal of Intelligent Material Systems and Structures*, 31(5):651–664.
14. Wapenaar, K. 2004. "Retrieving the Elastodynamic Green's Function of an Arbitrary Inhomogeneous Medium by Cross Correlation," *Physical review letters*, 93(25):254301.
15. Snieder, R. and E. Safak. 2006. "Extracting the building response using seismic interferometry: Theory and application to the Millikan Library in Pasadena, California," *Bulletin of the Seismological Society of America*, 96(2):586–598.
16. Kim, H. 2020. *Ultrasonic Guides Waves Test Method for Blunt Impact Damage Assessment on Composite Aircraft Structures*, Ph.D. thesis, University of California San Diego.